

---

# Princeton Plasma Physics Laboratory

---

PPPL-

PPPL-



Prepared for the U.S. Department of Energy under Contract DE-AC02-09CH11466.

# Princeton Plasma Physics Laboratory

## Report Disclaimers

---

### Full Legal Disclaimer

This report was prepared as an account of work sponsored by an agency of the United States Government. Neither the United States Government nor any agency thereof, nor any of their employees, nor any of their contractors, subcontractors or their employees, makes any warranty, express or implied, or assumes any legal liability or responsibility for the accuracy, completeness, or any third party's use or the results of such use of any information, apparatus, product, or process disclosed, or represents that its use would not infringe privately owned rights. Reference herein to any specific commercial product, process, or service by trade name, trademark, manufacturer, or otherwise, does not necessarily constitute or imply its endorsement, recommendation, or favoring by the United States Government or any agency thereof or its contractors or subcontractors. The views and opinions of authors expressed herein do not necessarily state or reflect those of the United States Government or any agency thereof.

### Trademark Disclaimer

Reference herein to any specific commercial product, process, or service by trade name, trademark, manufacturer, or otherwise, does not necessarily constitute or imply its endorsement, recommendation, or favoring by the United States Government or any agency thereof or its contractors or subcontractors.

---

## PPPL Report Availability

### Princeton Plasma Physics Laboratory:

<http://www.pppl.gov/techreports.cfm>

### Office of Scientific and Technical Information (OSTI):

<http://www.osti.gov/bridge>

---

### Related Links:

[U.S. Department of Energy](#)

[Office of Scientific and Technical Information](#)

[Fusion Links](#)

# Waves for Alpha-Channelling in Mirror Machines

A. I. Zhmoginov and N. J. Fisch

(Dated: June 18, 2009)

Alpha-channelling can, in principle, be implemented in mirror machines via exciting weakly-damped modes in the ion cyclotron frequency range with perpendicular wavelengths smaller than the alpha particle gyroradius. Assuming quasi-longitudinal or quasi-transverse wave propagation, we search systematically for suitable modes in mirror plasmas. Considering two device designs, a proof-of-principle facility and a fusion reactor prototype, we in fact identify candidate modes suitable for alpha-channelling.

## I. INTRODUCTION

Waves in the ion cyclotron range of frequencies can be employed in magnetic mirror plasmas for plasma production and heating [1–9], stabilization of plasma instabilities [10, 11], particle injection [12, 13], and plasma diagnostics [14–17]. Alpha-channelling is a recently proposed technique [18] for redirecting energy from  $\alpha$  particles to fusion ions by using waves to control the particle dynamics. Originally, the technique was proposed to avoid  $\alpha$  particle damping on waves used in rf current drive techniques [19], but the waves could also be used to extract energy from the  $\alpha$  particles. In particular, coupling certain rf waves in a tokamak or a mirror machine was predicted [18, 20–26] to induce  $\alpha$  particle flows in the phase space leading to quick  $\alpha$  ejection accompanied by  $\alpha$  particle cooling. As a result, the energy with which  $\alpha$  particles are born can be transferred to the waves and then used to sustain fusion reaction in the device. The channelling of the  $\alpha$  power in one simple mirror configuration [27] at ignition has been estimated [24] to increase, potentially, the effective fusion reactivity by a factor of 2.8.

In the absence of external electromagnetic fields, the free energy associated with energetic  $\alpha$  particles can feed numerous plasma instabilities, which can, in turn, transport energy to background plasma species [28–32]. The energy conversion rate in such processes was estimated [29] to be approximately 25%. This suggests that  $\alpha$ -channelling can potentially be a more effective energy transfer mechanism, also capable of fusion ash removal and fuel ion injection [24, 33].

The  $\alpha$ -channelling effect in a mirror machine was shown [24–26] to be possible, in principle, via arranging ion cyclotron wave regions along the device axis (Fig. 1) and adjusting their parameters. In our earlier work [33], the possibility of the  $\alpha$ -channelling effect in such systems was confirmed numerically by simulating  $\alpha$  particle motion in a magnetic mirror trap. In particular, we of-

fered a preliminary optimization of the device parameters and proposed a prototype configuration capable of extracting 60% of the trapped  $\alpha$  particle energy. However, the restrictions introduced on the wave dispersion by the plasma have not been addressed.

In this work, we analyze the dispersion relation of waves in mirror plasmas and search for the device parameters close to those of the optimum scheme [33]. We consider two different designs of a mirror machine, a proof-of-principle device and a fusion reactor prototype, and identify waves suitable for  $\alpha$ -channelling in both of them. We also show that such waves can be excited at different axial positions if the magnetic field profile has multiple local minima.

The paper is organized as follows. In Sec. II, we use two-dimensional ray-tracing equations to study wave propagation in the central cell of a mirror machine. Assuming that the wave propagates nearly parallel to the magnetic field lines, or in a transverse direction, we simplify equations describing the ray trajectory and propose a method of searching for waves suitable for  $\alpha$ -channelling. In Sec. III, following the approach outlined in Sec. II, we analyze the dispersion relation of plasmas

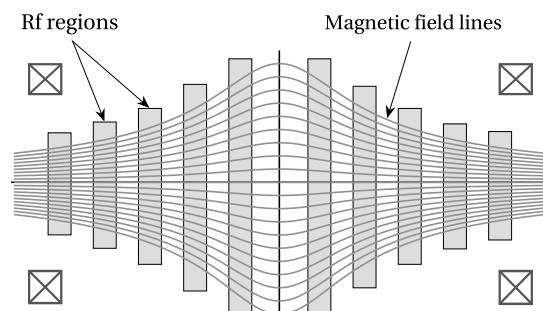


FIG. 1: Arrangement of rf regions (gray bars) in a mirror machine. These regions contain radially and axially localized azimuthally propagating waves in the ion cyclotron frequency range.

trapped in a mirror machine and search for modes with suitable parameters. After such modes are identified, we simulate ray trajectories numerically to show that the wave packet dynamics is consistent with the analytical predictions and that the identified modes are indeed suitable for  $\alpha$ -channeling. Section IV summarizes our conclusions. In Appendix A, we derive limitations on the wave parameters necessary for efficient  $\alpha$ -channeling.

## II. QUASI-LONGITUDINAL AND QUASI-TRANSVERSE WAVE PROPAGATION

As we show in Appendix A, the  $\alpha$ -channeling technique can be implemented in a mirror machine by exciting such electromagnetic waves in the ion-cyclotron frequency range, with  $k_{\parallel} \ll k_{\perp}$  and  $k_{\perp} \rho_{\alpha} \geq 1$ , that (a) they are weakly damped, and (b) the damping on electrons is much weaker compared to the damping on ions. In tokamaks, a leading candidate wave having this property was the mode converted ion Bernstein wave [34]. We now propose a method which can be used to identify waves satisfying these conditions in a mirror device.

### A. Ray-Tracing Equations

In this subsection, we write ray-tracing equations in the system of coordinates adjusted to the magnetic field lines. Considering wave propagation outside of the regions of strong damping, we assume that the device is large enough to fit many wavelengths so that the geometrical optics approximation is valid. Introducing a characteristic device length  $L$ , and a characteristic device diameter  $d \ll L$ , this condition can be rewritten as  $k_{\parallel} L \gg 1$  and  $k_{\perp} d \gg 1$ . Fixing azimuthal wave number  $m$ , two-dimensional ray trajectory  $\mathbf{r}(t)$ ,  $\mathbf{k}(t)$  can be obtained as a solution of the system [35]:

$$\frac{d\mathbf{r}}{d\tau} = \frac{\partial \mathcal{D}}{\partial \mathbf{k}}, \quad \frac{d\mathbf{k}}{d\tau} = -\frac{\partial \mathcal{D}}{\partial \mathbf{r}}, \quad (1)$$

where  $\mathcal{D} = 0$  is a wave dispersion relation,  $\mathbf{r} = (r, z)$  and  $\mathbf{k} = (k_r, k_z)$  are two-dimensional wave packet position and wave vector correspondingly, and  $\tau$  is the new independent variable, or ‘‘time’’ defined through

$$\frac{dt}{d\tau} = \frac{\partial \mathcal{D}}{\partial \omega}. \quad (2)$$

Consider  $\mathcal{D}$  as a function of  $k_{\parallel} = \mathbf{k} \cdot \hat{\mathbf{b}}$  and  $k_n = \mathbf{k} \cdot \hat{\mathbf{n}}$ , where  $\hat{\mathbf{b}}$  is a two-dimensional unit vector directed along

the magnetic field and  $\hat{\mathbf{n}}$  is a two-dimensional unit vector perpendicular to  $\hat{\mathbf{b}}$  such that  $n_r > 0$ ; then one can rewrite the ray-tracing equations as:

$$\dot{r} = \frac{\partial \mathcal{D}}{\partial k_{\parallel}} \hat{b}_r + \frac{\partial \mathcal{D}}{\partial k_n} \hat{b}_z, \quad (3)$$

$$\dot{z} = \frac{\partial \mathcal{D}}{\partial k_{\parallel}} \hat{b}_z - \frac{\partial \mathcal{D}}{\partial k_n} \hat{b}_r \quad (4)$$

$$\dot{k}_{\parallel} = -\hat{b}_r \left. \frac{\partial \mathcal{D}}{\partial r} \right|_{k_{\parallel}, k_n} - \hat{b}_z \left. \frac{\partial \mathcal{D}}{\partial z} \right|_{k_{\parallel}, k_n} + \frac{\partial \mathcal{D}}{\partial k_n} \left[ \frac{k_{\parallel}}{\rho_{\parallel}} + \frac{k_n}{\rho_{\perp}} \right], \quad (5)$$

$$\dot{k}_n = -\hat{b}_z \left. \frac{\partial \mathcal{D}}{\partial r} \right|_{k_{\parallel}, k_n} + \hat{b}_r \left. \frac{\partial \mathcal{D}}{\partial z} \right|_{k_{\parallel}, k_n} - \frac{\partial \mathcal{D}}{\partial k_{\parallel}} \left[ \frac{k_{\parallel}}{\rho_{\parallel}} + \frac{k_n}{\rho_{\perp}} \right], \quad (6)$$

where  $\rho_{\parallel}^{-1} = \hat{\mathbf{n}} \cdot [(\hat{\mathbf{b}} \nabla) \hat{\mathbf{b}}]$  is the magnetic field curvature, and  $\rho_{\perp}^{-1} = \hat{\mathbf{n}} \cdot [(\hat{\mathbf{n}} \nabla) \hat{\mathbf{b}}]$  is the curvature of lines in  $(r, z)$  plane transverse to the magnetic field lines. For convenience, we will further work in the system of coordinates adjusted to the magnetic field lines. In particular, instead of defining wave packet position  $(r, z)$  in cylindrical coordinates, we will characterize its position by a tuple  $(R, \eta)$ , where  $R \approx r \sqrt{B(\eta)/B_0}$  is a midplane distance from the system axis to the field line on which the wave packet resides,  $B_0 = B(0)$  is a midplane magnetic field and  $\eta$  is a coordinate along the field line such that  $\eta = 0$  on the midplane and  $d\eta = \hat{b}_z dz + \hat{b}_r dr$ .

### B. Quasi-Longitudinal Propagation

Assume that the group velocity of the wave packet is directed primarily along the magnetic field and that the radial gradients can be neglected. This makes negligible the term  $-\partial \mathcal{D} / \partial n \equiv -\hat{b}_z \partial \mathcal{D} / \partial r + \hat{b}_r \partial \mathcal{D} / \partial z$  in Eq. (6). In this case, the ray trajectory describes wave packets quickly moving along the magnetic field lines, while drifting slowly in  $R$ . Since  $R \ll L$ , the term proportional to  $\rho_{\parallel}^{-1}$  can be neglected compared to  $\rho_{\perp}^{-1}$ . Substituting  $\rho_{\perp}^{-1} \approx -(2B)^{-1} dB/d\eta$  in Eq. (6), one then obtains  $k_n = \zeta \sqrt{B}$ , where  $\zeta$  is a constant. As a result, longitudinal wave packet motion can be described by the Hamiltonian:

$$H(k_{\parallel}, \eta; \zeta, R) = \mathcal{D}(k_{\parallel}, k_n = \zeta \sqrt{B(\eta)}, \eta, R) = 0,$$

where  $k_{\parallel}$  is a canonical momentum,  $\eta$  is a canonical coordinate, and  $\zeta$ ,  $R$  are slowly changing parameters. To find how the  $k_{\parallel}(\eta)$  dependence evolves with time, note that since motion in  $(k_{\parallel}, \eta)$  space is fast compared to the transverse motion, the adiabatic invariant  $I_{\parallel} = \oint k_{\parallel} d\eta$  must be approximately conserved. This property and the knowledge of the slowly changing  $\zeta$  and  $R$  defines  $k_{\parallel}(\eta)$ . The evolution of  $\zeta$  and  $R$  can be calculated either using the following averaged equations:

$$\dot{\zeta} = - \left\langle \frac{1}{\sqrt{B}} \frac{\partial \mathcal{D}}{\partial n} \right\rangle, \quad \dot{R} = \left\langle \sqrt{B} \frac{\partial \mathcal{D}}{\partial k_n} \right\rangle,$$

where the averaging is performed over the fast longitudinal oscillations, or using the conservation of  $I_{\parallel}$  which restricts motion in  $(\eta, R)$  to a one-dimensional curve. A more strict derivation of these equations will be discussed in our future work.

If, for a wave of interest,  $k_{\parallel} \ll k_n$  and  $\eta \ll L$ , one can decompose

$$\mathcal{D} \approx \mathcal{D}_0(k_n, R) + \alpha(k_n, R)k_{\parallel}^2/2 + \beta(k_n, R)\eta^{2g}/2g, \quad (7)$$

where  $g$  is some integer number. Therefore, neglecting first order corrections with respect to  $k_{\parallel}$  and  $\eta$ , averaged motion in  $k_n$  and  $R$  satisfies  $\mathcal{D}_0(k_n, R) \approx 0$ . Substituting this solution in the expressions for  $\alpha(k_n, R)$  and  $\beta(k_n, R)$ , we can describe the shape of the longitudinal ray trajectory in  $(k_{\parallel}, \eta)$  space as the wave packet slowly drifts radially in the device.

Weakly damped longitudinal modes can be identified as closed loops on the graph  $k_{\parallel}(\eta; \zeta, R)$  which avoid regions of strong electron and ion Landau damping ( $\omega/k_{\parallel} \sim w_{e\setminus i}$ ) and regions of strong ion cyclotron damping [ $(\omega - n\Omega_i)/k_{\parallel} \sim w_i$ ], where  $w_s$  is a thermal velocity of the species  $s$ . We will further denote such loops as *candidate loops*. The value of  $k_{\parallel}$  solving  $H(k_{\parallel}, \eta; \zeta, R) = 0$  depends on  $\eta$  through longitudinal plasma parameter profiles. Neglecting effects associated with the longitudinal plasma temperature variation, and assuming that the line plasma density is nearly constant along a field line and hence  $n(\eta) \approx n_0 B(\eta)/B_0$ , one can express the longitudinal wave number as  $k_{\parallel}(B(\eta); \omega, m, \zeta, R\sqrt{B_0}, n_0/B_0, T_{e\setminus i})$ . Noticing this, one can plot  $k_{\parallel}(B)$  dependence for fixed parameter values and search for such  $B_0$  and the mirror ratio  $R_B$  that there is a loop on the  $k_{\parallel}(\eta)$  graph. Being plotted as a function of  $B$ , such loop can be located either in the middle of the segment  $[B_0, R_B B_0]$ , or be “wrapped” around one of its ends, in which case  $k_{\parallel}(B)$  graph restricted to  $B_0 \leq B \leq R_B B_0$  shows just a half of the loop.

In conclusion, in order to find a system which allows for a slowly damped longitudinally propagating wave trapped in it, one needs to study  $k_{\parallel}(B)$  dependencies plotted for different values of  $\omega$ ,  $m$ ,  $\zeta$ ,  $n/B$ ,  $r\sqrt{B}$ , and  $T$ . The features indicating existence of the mode include either a presence of the candidate loop, or a half of it located at  $B = B_0$ , or at  $B = R_B B_0$  for some  $B_0$  and  $R_B$ .

### C. Quasi-Transverse Propagation

Assume now that the wave of interest is instead propagating nearly perpendicular to the magnetic field lines. Since we suppose that the motion in  $(k_n, R)$  variables is fast, while the quiver motion in  $(k_{\parallel}, \eta)$  is negligible, the wave packet averaged motion along the magnetic field line can be described by

$$\dot{\eta} \approx \left\langle \frac{\partial \mathcal{D}}{\partial k_{\parallel}} \right\rangle, \quad (8)$$

$$\dot{k}_{\parallel} \approx - \left\langle \frac{\partial \mathcal{D}_0}{\partial \eta} \right\rangle + \left\langle k_n \frac{\partial \mathcal{D}_0}{\partial k_n} \right\rangle \frac{1}{\rho_{\perp}}, \quad (9)$$

where the averaging is performed over oscillations in  $(k_n, R)$  space. The quiver motion in  $(k_n, R)$  variables can be found independently using an approximate local dispersion relation  $\mathcal{D}(k_n, R; k_{\parallel}, \eta) = 0$  and  $\dot{R} = \partial \mathcal{D} / \partial k_n$ . Note that the slow motion in  $(k_{\parallel}, \eta)$  can also be found from the conservation of the adiabatic invariant  $I_{\perp}(k_{\parallel}, \eta) = \oint k_n(R; k_{\parallel}, \eta) dR$  associated with the fast oscillations.

To simplify Eqs. (8), (9), assume further that  $k_{\parallel} \ll k_n$  and that the transversely propagating wave is localized near the midplane at  $\eta \ll L$ . Decomposing again  $\mathcal{D} \approx \mathcal{D}_0(k_n, R) + \alpha(k_n, R)k_{\parallel}^2/2 + \beta(k_n, R)\eta^{2g}/2g$ , one approximates

$$\dot{\eta} \approx \langle \alpha \rangle k_{\parallel}, \quad (10)$$

$$\dot{k}_{\parallel} \approx - \langle \beta \rangle \eta^{2g-1} + g \left\langle \frac{\partial \mathcal{D}_0}{\partial k_n} k_n \right\rangle \frac{\eta^{2g-1}}{L^{2g}} = -\gamma \eta^{2g-1}. \quad (11)$$

If  $\langle \alpha \rangle \gamma > 0$ , Eqs. (10), (11) describe the particle motion in the attractive potential  $U(\eta) = \langle \alpha \rangle \gamma \eta^{2g}$ . Hence, the corresponding ray trajectories will be bounded in  $(k_{\parallel}, \eta)$  and under a proper choice of initial parameters they will be weakly damped on electrons due to  $k_{\parallel} \ll \omega/w_e$ . To identify such waves, one needs to study  $k_{\parallel}(B)$  dependencies and look for waves with  $k_{\parallel} \approx 0$ . If  $\langle \alpha \rangle \gamma > 0$  and the transverse motion of the found wave is quick compared

to the longitudinal motion, ray trajectory evolution in  $(k_{\parallel}, \eta)$  space satisfies Eqs. (10), (11), and such wave can be suitable for  $\alpha$ -channeling.

### III. NUMERICAL SIMULATIONS

To illustrate methods discussed in Sec. II and show that weakly damped modes can exist in practical fusion devices, we consider two mirror machine designs: a proof-of-principle facility and a fusion reactor prototype with parameters similar to those used in Refs. 36 and 37. We assume that the magnetic field  $\mathbf{B}$  in both devices is given by  $B_{\phi} = 0$ ,  $B_r = -r(dB_z/dz)/2$ , and

$$B_z = B_{\min} + \frac{1}{2}(B_{\max} - B_{\min})[1 - \cos(\pi |2\eta z/L|^g)],$$

where  $g$  is an integer,  $\eta \geq 1$  is a constant,  $B_{\min}$  and  $B_{\max}$  are the minimum and the maximum values of  $B_z$  correspondingly. We also assume that (i) the linear density of the plasma does not depend on the axial position, and hence  $n(z)|_{R=0} \approx n^0 B(z)/B_0$  on the axis, and (ii) that radial plasma temperature and density profiles are given by  $n(\mathbf{r}, z) = n(z)|_{R=0} \exp(-R^2/a^2)$  and  $T(\mathbf{r}) = T^0[\kappa + (1 - \alpha) \exp(-R^2/a^2)]$ , where  $\alpha \leq 1$  is a constant, and  $a$  is a characteristic plasma radius. The dispersion relation  $\mathcal{D} = 0$  is modelled by the plasma kinetic dispersion relation reading  $\mathcal{D} = \|\hat{\mathbf{e}} - n^2 \hat{\mathbf{i}} + \mathbf{n}\mathbf{n}\|$ , where  $\hat{\mathbf{e}} = \hat{\mathbf{i}} + \sum_s \hat{\chi}_s$ ,  $\hat{\chi}_s = \omega_{ps}^2/\omega \cdot \sum_n e^{-\lambda} \hat{\mathbf{Y}}_n^s(\lambda)$ , and tensor  $\hat{\mathbf{Y}}_n^s(\lambda)$  is given by the following expression [35]:

$$\hat{\mathbf{Y}}_n^s = \begin{pmatrix} \frac{n^2 I_n}{\lambda_s} A_n & -in \Delta I_n A_n & \frac{k_{\perp}}{\Omega_s} \frac{n I_n}{\lambda_s} B_n \\ in \Delta I_n A_n & Q A_n & \frac{ik_{\perp}}{\Omega_s} \Delta I_n B_n \\ \frac{k_{\perp}}{\Omega_s} \frac{n I_n}{\lambda_s} B_n & -\frac{ik_{\perp}}{\Omega_s} \Delta I_n B_n & \frac{2(\omega - n\Omega_s)}{k_{\parallel} w_{s\perp}^2} I_n B_n \end{pmatrix}.$$

Here  $\omega_{ps}^2$  is the plasma frequency for species  $s$ ,  $Q = (n^2 I_n \lambda_s^{-1} + 2\lambda_s \Delta I_n)$ ,  $\Delta I_n = I_n(\lambda_s) - I_n'(\lambda_s)$ ,  $A_n = (k_{\parallel} w_{s\parallel})^{-1} Z_0(\xi_n^s)$ ,  $B_n = k_{\parallel}^{-1} [1 + \xi_n^s Z_0(\xi_n^s)]$ ,  $\xi_n^s = (\omega - n\Omega_s)(k_{\parallel} w_{s\parallel})^{-1}$ ,  $\lambda_s = k_{\perp}^2 \rho_s^2/2$ ,  $Z_0$  is the real part of the plasma dispersion function,  $w_{s\parallel}$  and  $w_{s\perp}$  are parallel and perpendicular thermal particle velocities correspondingly,  $\rho_s = w_{s\perp}/\Omega_s$ , and  $\Omega_s$  is the gyrofrequency.

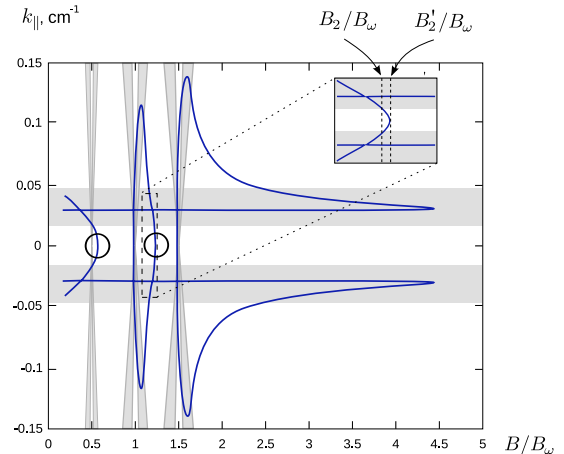


FIG. 2: Dependence of  $k_{\parallel}$  on  $B/B_{\omega}$  for  $\omega \approx 5.8 \times 10^7 \text{ s}^{-1}$ ,  $r\sqrt{B} = 18.3 \text{ cm} \times \text{T}^{1/2}$ ,  $n_D^0/n_T^0 = 1$ ,  $n/B = 6.67 \times 10^{12} \text{ cm}^{-3} \text{T}^{-1}$ ,  $m = 1$ , and  $\zeta = 0.045 \text{ cm}^{-1} \text{T}^{-1/2}$ . Parts of the dispersion curve lying inside the gray areas correspond to waves strongly damped through electron Landau resonance, or ion cyclotron resonance. Circles indicate the parts of the dispersion curve in the regions  $[B_{1\setminus 2}/B_{\omega}, B'_{1\setminus 2}/B_{\omega}]$  corresponding to the weakly-damped mode candidates. The inset shows zoomed in band  $[B_2/B_{\omega}, B'_2/B_{\omega}]$  in better resolution.

#### A. Dependence $k_{\parallel}(B)$ for the Proof-of-Principle Facility

For a proof-of-principle facility [36, 37] consider an open system with characteristic diameter  $d = 6a = 1.2 \text{ m}$ , the central cell length  $L = 12 \text{ m}$ , ion and electron temperatures on the axis  $T_e^0 = T_i^0 = 4 \text{ keV}$ ,  $\kappa = 0.15$ ,  $B \sim 1 \text{ T}$ , the electron and ion densities on the axis at the mid-plane  $n_e^0 = n_D^0 + n_T^0$  being of order of  $10^{13} \text{ cm}^{-3}$  with  $n_D^0$  and  $n_T^0$  being the deuterium and tritium densities correspondingly.

Consider first the case  $k_{\perp} \rho_{\alpha} \sim 1$ , or  $k_{\perp} \rho_i \ll 1$ . Calculating the dependence  $k_{\parallel}(B)$  numerically for  $r\sqrt{B} = 18.3 \text{ cm} \times \text{T}^{1/2}$ ,  $n_D^0/n_T^0 = 1$ ,  $n/B = 6.67 \times 10^{12} \text{ cm}^{-3} \text{T}^{-1}$ ,  $m = 1$ ,  $\zeta = 0.045 \text{ cm}^{-1} \text{T}^{-1/2}$ , and  $\omega \approx 5.8 \times 10^7 \text{ s}^{-1}$  approximately equal to the deuterium gyrofrequency in the magnetic field  $B_{\omega} = 1.2 \text{ T}$ , several loop candidates were identified (Fig. 2). Both parts of the plot indicated by circles lie outside of the areas amenable to strong Landau and ion cyclotron damping and have reflection points at the higher values of the magnetic field. Hence, both these curve segments described by an approximate dispersion relation

$$a = n_{\parallel}^2 + \frac{d^2}{b - n^2}, \quad (12)$$

where

$$a \approx 1 - \sum_i \frac{\omega_{pi}^2}{\omega} \sum_n e^{-\lambda_i} \frac{n^2 I_n(\lambda_i)}{\lambda_i (\omega - n\Omega_i)},$$

$$b \approx 1 - \sum_i \frac{\omega_{pi}^2}{\omega} \sum_n \frac{e^{-\lambda_i}}{\omega - n\Omega_i} \left[ \frac{n^2 I_n(\lambda_i)}{\lambda_i} + 2\lambda_i (I_n - I'_n) \right],$$

$$d \approx \sum_i \frac{\omega_{pi}^2}{\omega} \sum_n \frac{ne^{-\lambda_i} (I_n - I'_n)}{\omega - n\Omega_i} + \frac{\omega_{pe}^2}{\omega\Omega_e},$$

might correspond to weakly-damped modes trapped near the midplane. This dispersion relation was derived from  $\|\hat{\mathbf{e}} - n^2 \hat{\mathbf{i}} + n\mathbf{n}\| = 0$  neglecting  $n_\perp^2$  compared to  $\varepsilon_{zz}$ , neglecting  $\varepsilon_{xz}$ ,  $\varepsilon_{zx}$ ,  $\varepsilon_{xy}$ ,  $\varepsilon_{yx}$ , and assuming that  $\Omega_e \gg \omega$ . The dispersion relation (12) is the finite- $k_\perp \rho$  version of the fast wave dispersion relation for cold plasmas reading  $(S - n_\parallel^2)(S - n^2) = D^2$ , where

$$S = 1 + \sum_s \frac{\omega_{ps}^2}{\Omega_s^2 - \omega^2},$$

$$D = \sum_s \frac{\omega_{ps}^2 \Omega_i}{\omega(\Omega_s^2 - \omega^2)}.$$

However, while Eq. (12) describes both observed waves with  $k_\parallel \approx 0$  shown in Fig. 2, the cold dispersion relation holds only at  $\omega \approx \Omega_D$ . Considering this wave, the mode characteristic growth rate  $\gamma$  which is attributed to the interaction with  $\alpha$  particles can be estimated as:

$$\gamma \sim \omega_{p\alpha}^2 \frac{\Delta\eta}{v_{\parallel \text{res}}} \frac{w_{\alpha\perp}}{v_{\parallel \text{res}}},$$

where  $\omega_{p\alpha}$  is the  $\alpha$  particle plasma frequency,  $\Delta\eta$  is the characteristic length of the rf region,  $v_{\parallel \text{res}} = (\omega - n\Omega_\alpha)k_\parallel^{-1}$  is the resonant parallel velocity, and  $n$  is the cyclotron resonance number. The derivation of this result will be discussed in our future works.

Notice that for both loop candidates shown in Fig. 2  $k_\parallel \ll k_n$  and that they can exist in the local minimum of the magnetic field only. Numerical calculations of  $k_\parallel(B)$  dependence for other wave and plasma parameters different from those used in Fig. 2 by no more than one order of magnitude, did not reveal any candidate waves which either had  $k_\parallel \gtrsim k_n$ , or were represented by closed loops in  $k_\parallel(B)$  plot. Hence, for  $k_\perp \rho_i \ll 1$ , the observed candidate waves can be studied assuming quasi-longitudinal, or quasi-transverse propagation and using Eq. (7). Furthermore, in performing numerical calculations of  $k_\parallel(B)$

dependence for  $k_\perp \rho_i \gtrsim 1$  for plasma and wave parameters similar to those used in  $k_\perp \rho_i \ll 1$  case, we also did not observe candidate waves with  $k_\parallel \gtrsim k_n$ , or closed loops in the  $k_\parallel(B)$  plot. This suggests that the candidate waves with  $k_\perp \rho_i \gtrsim 1$  can be studied using the same approach used for the waves with  $k_\perp \rho_i \gtrsim 1$ .

## B. Quasi-Longitudinal and Quasi-Transverse Waves in the Proof-of-Principle Facility

We now study wave candidates similar to those shown in Fig. 2. We assume that the corresponding waves propagate either quasi-longitudinally, or quasi-transversely and that for such waves  $k_\parallel \ll k_n$  and  $\eta \ll L$ . Using Eq. (7), one obtains approximate expression for the wave packet trajectory in  $(k_n, R)$  space:

$$\mathcal{D}_0(k_n, R) \approx 0.$$

The numerical solution of this equation for  $\omega \approx 5.8 \times 10^7 \text{ s}^{-1}$ ,  $T_e^0 = T_i^0 = 4 \text{ keV}$ ,  $n_e^0 \approx 7.4 \times 10^{12} \text{ cm}^{-3}$ ,  $n_D^0/n_T^0 = 1$ ,  $\kappa = 0.15$ ,  $m = 1$ , and  $B \approx 1.5 \text{ T}$  is shown on Fig. 3. According to this figure, there are two distinct trajectories in  $(k_n, R)$  space, for one of which, marked with “s”, the characteristic period of motion  $T_s$  is of order of  $10T_l$ , while for another, marked with “f”, the period of motion  $T_f$  is of order of  $0.02T_l$ . Here  $T_l$  is a characteristic period of the longitudinal motion calculated for the ray trajectory with  $k_\parallel \sim 0.004 \text{ cm}^{-1}$ . Since  $T_f \ll T_l \ll T_s$ , the trajectory marked with  $s$  corresponds to the longitudinal wave propagation, while the trajectory marked with  $f$  corresponds to the transverse case. An example of a ray trajectory plotted for the longitudinal case is shown on Fig. 4. According to this figure, which captures one period of slow motion in  $(k_n, R)$ , the parallel adiabatic invariant  $I_\parallel$  is nearly conserved. Due to  $I_\parallel$  conservation, the maximum value of  $k_\parallel$  is reached near the point of the curve  $\mathcal{D}_0(k_n, R) = 0$ , where  $\beta/\alpha$  reaches maximum. For the parameters used to plot Fig. 4, the minimum of  $v_{\text{ph}}/w_e = \omega/(k_\parallel w_e)$  is approximately equal to 3 and, therefore, the corresponding wave is weakly damped on electrons.

For the transversely propagating wave, there exist two possible regimes. In one of them, shown in Fig. 5 with a dashed line, the characteristic reflection time, on which  $k_\parallel$  changes sign, is of order of  $T_f$ . In this regime, the description of the longitudinal motion by particle motion in the potential  $U(\eta) = \langle \alpha \rangle \gamma \eta^{2g}$  is inaccurate. Instead, there will be a random walk in  $k_\parallel$  as a result of

which a wave packet can approach  $k_{\parallel} \sim \omega/w_e$  and become strongly damped on electrons. In another regime shown in Fig. 5 with a solid line, the characteristic reflection time is much larger than  $T_f$ . In this case, the ray trajectory can be described by the equations of motion in the potential  $U(\eta) = \langle \alpha \rangle \gamma \eta^{2g}$  and, as a result, such wave can remain weakly damped after many longitudinal oscillations.

To provide examples of the modes weakly damped on electrons, but interacting with deeply trapped  $\alpha$  particles, we considered several system designs. The best result for  $k_{\perp\rho_i} \ll 1$  case was achieved for the system with  $\omega \approx 5.8 \times 10^7 \text{ s}^{-1}$ ,  $T_e^0 = T_i^0 = 4 \text{ keV}$ ,  $n_e^0 \approx 4.2 \times 10^{12} \text{ cm}^{-3}$ ,  $n_D^0/n_T^0 = 1$ ,  $m = 1$ , and  $B \approx 0.6 \text{ T}$ . In this configuration,  $\omega \approx 2\Omega_D$  and the interaction with  $\alpha$  particles occurs through the second cyclotron resonance. The quasi-transverse wave launched near the midplane at  $R = 20 \text{ cm}$  and having initial  $k_{\parallel} \sim 0.005 \text{ cm}^{-1}$  was shown to be weakly damped on electrons since  $\min v_{\text{ph}}/w_e \approx 3.5$  and strongly interacting with  $\alpha$  particles because  $\min v_{\text{res}}/w_{\alpha} \approx 0.34$ , where  $v_{\text{res}}$  is a resonance parallel velocity calculated for  $n = 2$ . The mode was also shown to be bounded radially and longitudinally in a region with  $\Delta R \sim 30 \text{ cm}$  and  $\Delta \eta \sim 4 \text{ m}$ . The characteristic values of  $k_n \Delta R$  and  $k_{\parallel} \Delta \eta$  were approximately equal to 2.5, and hence, such wave can, in principle, be excited in a device

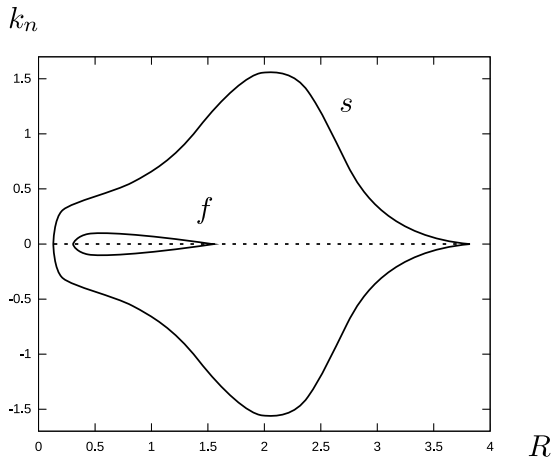


FIG. 3: Solution of equation  $\mathcal{D}_0(k_n, R) = 0$  for  $\omega \approx 5.8 \times 10^7 \text{ s}^{-1}$ ,  $T_e^0 = T_i^0 = 4 \text{ keV}$ ,  $n_e^0 \approx 7.4 \times 10^{12} \text{ cm}^{-3}$ ,  $\kappa = 0.15$ ,  $n_D^0/n_T^0 = 1$ ,  $m = 1$ , and  $B \approx 1.5 \text{ T}$ . The slow trajectory, period of motion along which is much larger than the characteristic period of the longitudinal oscillations, is marked with letter “s”. The fast trajectory is marked with letter “f”. The period of oscillations along this trajectory is much smaller than the characteristic period of the longitudinal motion.

of a similar size. Interestingly, both  $k_n \Delta R$  and  $k_{\parallel} \Delta \eta$  can be increased for fixed device scale sizes and  $B_0$  by considering higher cyclotron resonances. Numerical simulations confirmed that after doubling  $\omega$  (so that  $\omega \approx 4\Omega_D$ ), not only the characteristic  $k_{\parallel}$  can be doubled while leaving  $\omega/(k_{\parallel} w_e)$  the same as for  $\omega \approx 2\Omega_D$ , but the maximum  $k_n$  achieved for the quasi-transverse wave is also nearly doubled. As a result,  $k_n \Delta R$  increased nearly three times (due to both  $k_n$  and  $\Delta R$  increase), while  $k_{\parallel} \Delta \eta$  increased more than twice.

In  $k_{\perp\rho_i} \gg 1$  case, we considered quasi-longitudinal modes in the system with  $\omega \approx 5.8 \times 10^7 \text{ s}^{-1}$ ,  $T_e^0 = T_i^0 = 4 \text{ keV}$ ,  $n_e^0 \approx 7.6 \times 10^{12} \text{ cm}^{-3}$ ,  $n_D^0/n_T^0 = 1$ ,  $m = 20$ , and  $B \approx 1.15 \text{ T}$ . The wave was launched close to the device periphery at  $R = 55 \text{ cm}$  with initial  $k_{\parallel} \sim 0.006 \text{ cm}^{-1}$  and was shown to be weakly damped on electrons since  $\min v_{\text{ph}}/w_e \approx 3.5$  and strongly interacting with  $\alpha$  particles because  $\min v_{\text{res}}/w_{\alpha} \approx 0.42$ . The mode was bounded both radially with  $\Delta R \sim 60 \text{ cm}$  and longitudinally with  $\Delta \eta \sim 6 \text{ m}$ . Since  $k_n$  reaches 15.0 along the ray trajectory, the radial wave number of the mode is very large and  $\max k_{\perp\rho_{\alpha}} \approx 300$ . The characteristic value  $k_{\parallel} \Delta \eta$ , in turn, was approximately equal to 4, and hence, such mode can, in principle, be excited in the proof-of-principle device.

As an intermediate conclusion, two qualitatively different weakly damped modes with  $k_{\perp\rho_D} \ll 1$  and  $k_{\perp\rho_D} \gg 1$ , with  $\tau_i \gg \tau_e$ , capable of resonant interaction with deeply-trapped  $\alpha$  particles, have been identified.

### C. Fusion Reactor Prototype

For a fusion reactor prototype, following Ref. 36, we consider a mirror machine with the following parameters:  $d = 6 \text{ m}$ ,  $L = 15 \text{ m}$ ,  $B_0 = 3 \text{ T}$ ,  $n_e^0 = n_D^0 + n_T^0 \approx 10^{14} \text{ cm}^{-3}$ ,  $T_e = 60 \text{ keV}$ , and  $T_i = 15 \text{ keV}$ . Even though  $w_e \approx 0.2c$ , we neglected relativistic effects and used the same dispersion relation as in Sec. III A. Similarly to the proof-of-principle facility, the dependencies of  $k_{\parallel}$  on  $B$  did not show any candidate waves which either had  $k_{\parallel} \gtrsim k_n$ , or were represented by closed loops on  $k_{\parallel}(B)$  plot. Numerical simulations confirmed that, by analogy with the proof-of-principle facility, in the prototype device, two weakly damped modes capable of resonant interaction with deeply-trapped  $\alpha$  particles,  $\tau_i \gg \tau_e$ , and either  $k_{\perp\rho_D} \ll 1$  (quasi-transverse wave), or  $k_{\perp\rho_D} \gg 1$  (quasi-longitudinal wave) could be identified. However, since in the fusion reactor prototype,  $\omega L/w_e$  is 1.3 times smaller compared to the proof-of-principle facility, we used higher

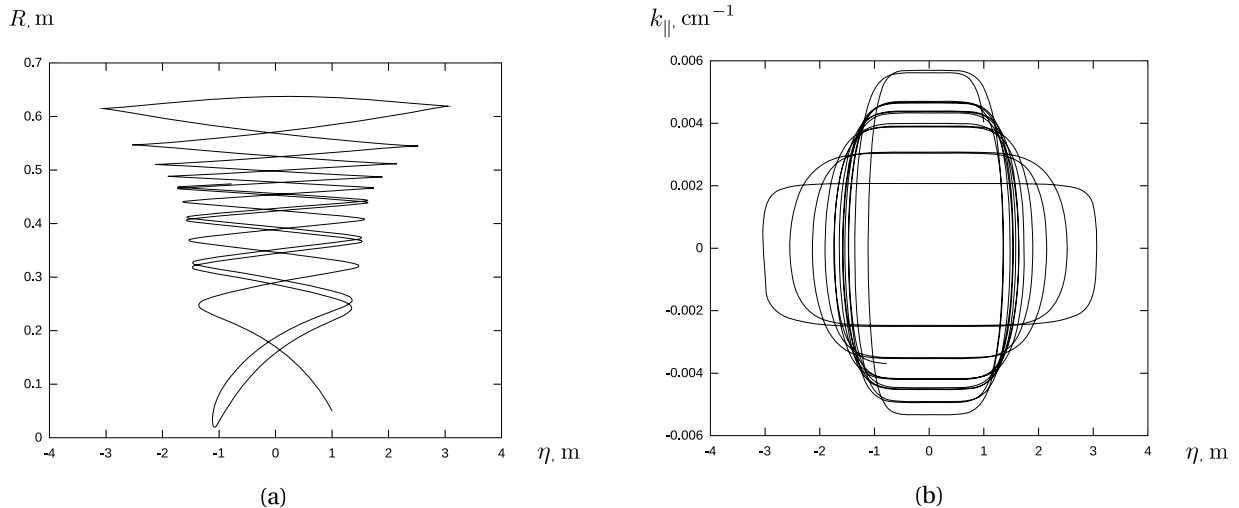


FIG. 4: Ray trajectory plotted for the longitudinally propagating wave: (a) ray trajectory in  $(k_{\parallel}, \eta)$  space, (b) ray trajectory in  $(r, z)$  coordinates. The system parameters are  $\omega \approx 5.8 \times 10^7 \text{ s}^{-1}$ ,  $T_e^0 = T_i^0 = 4 \text{ keV}$ ,  $n_e^0 \approx 7.4 \times 10^{12} \text{ cm}^{-3}$ ,  $n_D^0/n_T^0 = 1$ ,  $\kappa = 0.15$ ,  $m = 1$ ,  $B_{\min} \approx 1.5 \text{ T}$ ,  $B_{\max} = 5B_{\min}$ . The ray is launched from the point with  $k_{\parallel}^0 = 0.004 \text{ cm}^{-1}$  and  $\eta = 1 \text{ m}$ .

ion cyclotron resonances to satisfy both  $k_{\parallel} \Delta \eta \gtrsim \pi$  and  $k_n \Delta R \gtrsim \pi$ .

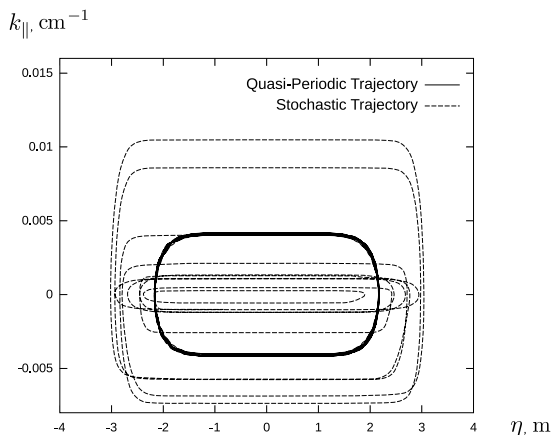


FIG. 5: Ray trajectories in  $(k_{\parallel}, \eta)$  space for two quasi-transverse waves: (i) chaotic trajectory plotted for the case  $T_f \sim T_r$  (dashed), where  $T_r$  is a characteristic  $k_{\parallel}$  reflection time, (ii) quasi-periodic trajectory for  $T_f \ll T_r$  (solid). Both trajectories are simulated for the system with  $\omega \approx 5.8 \times 10^7 \text{ s}^{-1}$ ,  $m = 1$ ,  $\kappa = 0.15$ ,  $n_e^0 \approx 9.8 \times 10^{12} \text{ cm}^{-3}$ ,  $B_{\min} \approx 1.5 \text{ T}$ , and  $B_{\max} = 5B_{\min}$ . The random walk occurs in a system with  $T_e^0 = T_i^0 = 4 \text{ keV}$  and  $n_T/n_D = 1$ , while the quasi-periodic trajectory is plotted for the case  $T_e^0 = T_i^0 = 2 \text{ keV}$  and  $n_T/n_D = 1.5$ .

#### D. Multiple Wave Regions

The system of rf regions with high  $\alpha$ -channeling efficiency, proposed in Ref. [24, 25], consisted of several waves located at different axial positions. Unfortunately, the weakly-damped mode described by the dispersion relation (12) was shown to exist only in a small vicinity of the local magnetic field minimum and hence could not be employed anywhere except at the midplane. In order to use the mode described by Eq. (12) for  $\alpha$ -channeling at an arbitrary axial position, a magnetic field profile with several minimum- $B$  wells can be employed. For example, the  $k_{\parallel}(\eta)$  dependencies for two waves with equal values of  $k_{\perp}$ , but different values of  $\omega$ , with the magnetic field profile illustrated in Fig. 6a, is shown in Fig. 6b. Three weakly-damped ion-cyclotron modes, one at the midplane, and others at  $|z| = z_m$ , exist in such a configuration and are shown in Fig. 6b with arrows.

#### IV. DISCUSSION

We described the limitations on the wave parameters necessary to achieve a high  $\alpha$ -channeling efficiency. In particular, ion-cyclotron waves weakly damped on electrons and having  $k_{\parallel} \ll k_{\perp}$ ,  $k_{\perp} \rho_{\alpha} \geq 1$  are considered suitable for  $\alpha$ -channeling. Assuming that such waves propagate either along the magnetic field lines, or perpendicular to them, we proposed an algorithm to identify modes with desired properties in a given mirror machine config-

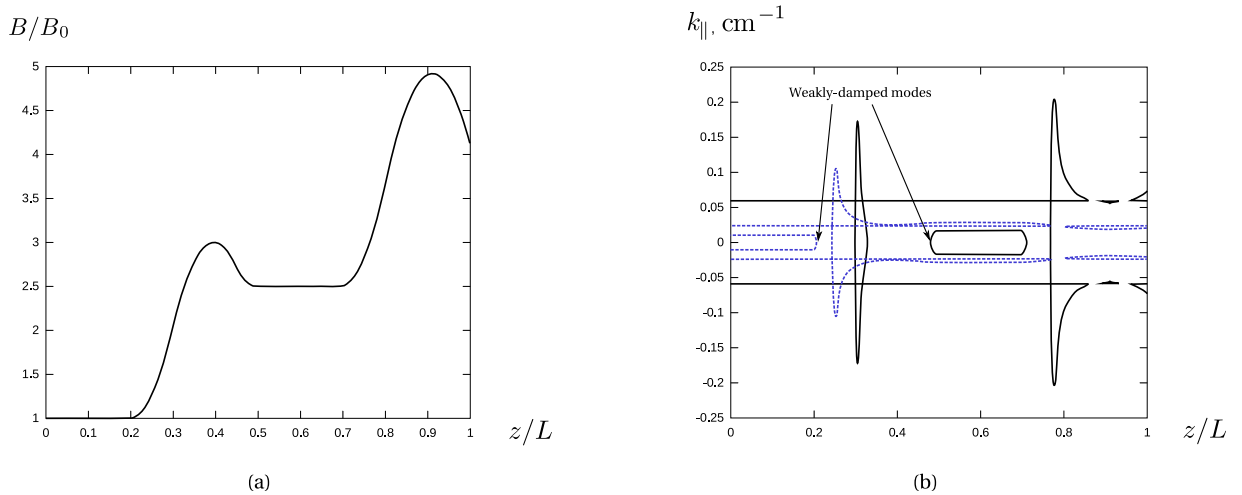


FIG. 6: (a) The magnetic field profile in a system with three magnetic field wells. One well is near the midplane at  $z = 0$  and the other two are at  $|z| = z_m \approx 0.6L$ . (b) The dependence  $k_{\parallel}(z/L)$  for two waves with  $\omega_1 \approx 0.8\Omega_D^0$  (dashed) and  $\omega_2 \approx 2\Omega_D^0$  (solid), where  $\Omega_D^0$  is a deuterium gyrofrequency at the midplane. Three weakly-damped modes located near  $z = 0$  and  $|z| = z_m$  are indicated with arrows.

uration. In order to find weakly-damped modes, we both (i) looked for waves with  $k_{\parallel} \approx 0$  and (ii) analyzed the dependence of  $k_{\parallel}$  on  $B$ , looking for closed loops, or half of closed loops located away from regions subjected to strong Landau or ion cyclotron damping. This method was applied to two mirror machine designs: a proof-of-principle facility and a fusion reactor prototype.

As a result, we were able to identify mode candidates suitable for  $\alpha$ -channeling in both devices. By simulating a two-dimensional ray trajectory, we confirmed the validity of the method and showed that there exist weakly-damped fast waves localized both radially and axially for which  $k_{\parallel}$  is always smaller than any pre-chosen value. These modes were shown to be interacting with deeply trapped  $\alpha$  particles, while being weakly damped on electrons and even more weakly damped on ions. Furthermore, in order to improve prospects of the weakly-damped mode excitation for  $\alpha$ -channeling in mirror machines, a possibility to arrange several rf regions at different axial positions using magnetic field profile with several wells was demonstrated.

The fact that modes suitable for  $\alpha$ -channeling exist does not yet mean that a complete scenario has been demonstrated. It does remain to determine the fraction of affected  $\alpha$  particles and the expected  $\alpha$ -channeling efficiency. Furthermore, methods used to find waves suitable for  $\alpha$ -channeling do not exhaust all possibilities. Moreover, the plasma configuration considered is simple; more complicated configurations of plasma may permit other

wave candidates. Thus, while an extensive search of suitable waves was conducted here, other candidate modes, possibly superior to the ones identified here, may in fact exist, and remain to be discovered.

## V. ACKNOWLEDGMENTS

This work was supported by DOE Contracts No. DE-FG02-06ER54851 and DE-AC0276-CH03073.

### Appendix A. Restrictions on Wave Parameters

The  $\alpha$ -channeling effect is a phenomenon in the phase space  $(\mathbf{r}, \mathbf{p})$ , in which  $\alpha$  particles born at fusion reactions diffuse along one-dimensional paths due to resonant interaction with electromagnetic waves imposed over a background dc magnetic field. If the diffusion induced along the path is suppressed at high energy whereas at the low-energy end there is an effective particle “sink”, the interaction with the waves will result in the ejection of the cold  $\alpha$  particles from the system and simultaneous transfer of their initial energy to the waves. The  $\alpha$  particle ejection leads to fusion ash removal, while by coupling the amplified wave to ion species, it is possible to redirect extracted energy to fuel ions, thus increasing effective fusion reactivity compared to the typical scenario, in which born  $\alpha$  particles heat plasma, slowing down collisionally on electrons.

Considering the wave- $\alpha$  particle interaction and the wave damping on ions and electrons independently, we will now derive the limitations on the wave parameters necessary to maximize the energy transfer from  $\alpha$  particles to fuel ions. In particular, we show that weakly damped electromagnetic waves in the ion-cyclotron frequency range, with  $k_{\parallel} \ll k_{\perp}$ ,  $k_{\perp}\rho_{\alpha} \geq 1$ , and weaker damping on electrons compared to damping on ions, are suitable for  $\alpha$ -channeling.

### A. Diffusion Path Shape

The diffusion path can be seen from the Hamiltonian of a particle moving in a homogeneous background magnetic field and a field of a plane wave reading

$$H = \frac{(\mathbf{p} - q\mathbf{A}_0/c - q\mathbf{A}_{\sim}/c)^2}{2M} + q\varphi_{\sim}, \quad (13)$$

where  $q$  and  $M$  are the particle charge and mass, correspondingly,  $\varphi_{\sim}$  and  $\mathbf{A}_{\sim}$  are scalar and vector potentials of the electromagnetic wave, and  $\mathbf{A}_0$  is a vector potential of the background dc magnetic field  $\mathbf{B} = \hat{z}B$  with  $\hat{z}$  being a unit vector directed along the  $z$  axis.

First we derive the resonance condition. Assuming that the wave field is weak, one can find the particle trajectory using Hamiltonian perturbation theory [38], treating terms proportional to  $\mathbf{A}_{\sim}$  and  $\varphi_{\sim}$  as weak perturbations to the unperturbed Hamiltonian  $H_0 = (\mathbf{p} - q\mathbf{A}_0/c)^2/(2M)$ . According to KAM theorem [38], the invariant tori of the unperturbed problem located near the resonances  $\omega - n\Omega - k_z v_z = 0$ , where  $\omega$  is a wave frequency,  $\Omega$  is a cyclotron frequency,  $\mathbf{k}$  is a wave vector,  $\mathbf{v}$  is a particle velocity, and  $n$  is an arbitrary integer number, are destroyed. Fixing  $\Omega$ ,  $n$  and  $\alpha$  particle parallel resonant velocity  $v_z^0$ , the resonance condition can be understood as a relation between the required  $\omega$  and  $k_z$ .

The shape of the diffusion path can be derived from Eq. (13). Since  $\varphi_{\sim}$  and  $\mathbf{A}_{\sim}$  depend on time through the wave phase  $\omega t - \mathbf{k}\mathbf{r}$ , as a result of a canonical transformation to a new longitudinal coordinate  $\kappa = z - \omega t/k_z$ , new Hamiltonian  $\mathcal{H}$  will be independent of time and will take the form:

$$\mathcal{H} = \frac{(\mathbf{P} - q\mathbf{A}(x, y, \kappa)/c)^2}{2M} + q\varphi(x, y, \kappa) - P_z\omega/k_z,$$

where  $\mathbf{A} = \mathbf{A}_0 + \mathbf{A}_{\sim}$ ,  $\mathbf{P}$  is a new canonical momentum, and  $\kappa$  is a new longitudinal canonical coordinate. Introducing the kinetic particle momentum  $\mathbf{p} = M\dot{\mathbf{r}}$ , and

using  $A_{0z} = 0$ , the conservation of  $\mathcal{H}$  leads to:

$$\frac{p_{\perp}^2}{2M} + \frac{(p_z - M\omega/k_z)^2}{2M} + q\varphi - \frac{q\omega}{ck_z}A_{\sim z} = \text{const},$$

where  $p_{\perp}^2 = p_x^2 + p_y^2$ . Therefore, a particle resonantly interacting with the wave diffuses along a one-dimensional path defined by the equation  $p_{\perp}^2 + (p_z - m\omega/k_z)^2 = \text{const}$  describing a circle in  $(p_{\perp}, p_z)$  space. To keep the wave in resonance with the particle while it moves along the path, parallel particle velocity should remain nearly constant, what is achieved when  $k_z v_{\perp} \ll \omega$ . If another condition  $k_{\perp}\rho_{\alpha} = \rho_{\alpha}\sqrt{k_x^2 + k_y^2} \geq 1$  is satisfied, this limitation can be rewritten as  $k_z \ll nk_{\perp}$ . Note, however, that if  $k_z \gtrsim nk_{\perp}$  and  $k_z$  depends on  $z$ , diffusion of a particle repeatedly interacting with a wave will be accompanied by a change of  $v_z$  and thus the change of the position where the resonance condition  $\omega - n\Omega - k_z v_z = 0$  is satisfied. This effect accompanied by a proper choice of the wave longitudinal profile can be considered a useful tool for manipulating particle diffusion along the path, but will not be studied in this work.

### B. Suppression of the Diffusion Along the Path

A limitation on  $k_{\perp}$  value follows from the analysis of the particle diffusion. The quasilinear diffusion equation written along the resonant path for a homogeneous magnetic field reads [39]

$$\frac{\partial p}{\partial t} = \frac{\partial}{\partial l} \left( D_l \frac{\partial p}{\partial l} \right), \quad (14)$$

where  $D_l$  is a diffusion coefficient,  $l$  is a linear coordinate along the diffusion path in the multi-dimensional action variable space of the unperturbed problem and  $p(l; t)$  is a particle density on the path. The action variables of the unperturbed problem are the parallel momentum  $p_{\parallel}$ , the magnetic moment  $\mu = mv_{\perp}^2/2B$ , negative particle energy  $-H$ , and  $m\Omega X$ , where  $X$  is an  $x$  component of the particle guiding center [40]. Notice that if at some point  $l = l_0$ ,  $D_l(l)$  vanishes, particles cannot diffuse past such a point [41]. This effect is particularly important for limiting  $\alpha$  particle heating and hence reducing average  $\alpha$  particle extraction time. The optimal value of  $l_0$  should be greater than  $l = l_b$ , where  $\alpha$  particles are born, but it cannot be much greater than  $l_b$  either, because this would result in heating of particles. If there is only one wave resonant with a given  $\alpha$  particle, the condition  $l_0 \gtrsim l_b$  limits  $k_{\perp}\rho_{\alpha}(l_b)$ . For example, for an electrostatic wave,

$D_E \sim J_n^2(k_\perp \rho_\alpha)$ , where  $D_E$  is a characteristic energy-space diffusion coefficient and  $J_n$  is the Bessel function of order  $n$ . This suggests that  $k_\perp \rho_\alpha(l_b)$  should be somewhat less than the first positive zero of the Bessel function  $J_n(x)$ .

If there are several uncorrelated waves with identical  $k_z$  and  $\omega$ , but different transverse wavenumbers  $k_\perp i$ , the diffusion along the path is not suppressed by previously discussed effects, but it can be avoided by the radial limitation of the wave. If for every  $i$  and  $j$ , one has  $|k_\perp i - k_\perp j| \ll k_\perp i$ , finite excursion of the particle energy  $\Delta E$  leads to a particle radial excursion  $\Delta r \sim -k_\perp \Delta E (m_\alpha \omega \Omega_\alpha)^{-1} \sim -k_\perp \rho_\alpha^2 / n$ , where  $m_\alpha$  is the  $\alpha$  particle mass, and  $k_\perp$  is an average of  $k_\perp i$ . Thus, by choosing  $k_\perp \rho_\alpha(l_b) \gg 1$ , which allows radial displacements much larger than  $\rho$ , and by limiting radial wave profile,  $\alpha$  particle heating is constrained by the maximum possible radial excursion before the particle leaves the wave.

### C. Required Wave Damping Rates

Efficient  $\alpha$ -channeling is possible only if the wave amplitude is much larger than a certain critical value  $f_0$  at which the characteristic  $\alpha$  particle extraction time  $\tau_{\text{extr}}$  is of order of the typical collisional  $\alpha$ -electron energy re-

laxation time  $\tau_{\alpha e}$ . But even if  $\tau_{\text{extr}} \gg \tau_{\alpha e}$ , electrons can gain more energy than ions if the wave damping on electrons is stronger than the wave damping on ions. Therefore, we will further focus our attention on waves with  $\tau_e \gg \tau_i$ , where  $\tau_s$  is a characteristic Landau or ion-cyclotron wave damping time on species  $s$ . If for some wave  $\tau_i \geq \tau_e$ , we will assume that there exist another mechanism which can transport wave energy to ions on the characteristic time scale further denoted by the same  $\tau_i$ , which is much smaller than  $\tau_e$ .

Another limitation on  $\tau_i$  follows from the fact that the  $\alpha$ -channeling technique is practical only if the energy extracted from  $\alpha$  particles exceeds the energy necessary to excite the channeling wave. In particular,  $\tau_i$  must be larger than the time  $\tau_{\text{amp}}$  on which the wave amplitude is amplified by a factor of 2. Assuming that the geometrical optics approximation is valid, a dimensionless parameter  $\xi = \tau_{\text{amp}} / \tau_L$ , where  $\tau_L$  is a time which takes the wave packet to travel a distance comparable to the device length  $L$ , can be introduced. If the rate of  $\alpha$  particle production is so large that  $\xi \ll 1$ ,  $\alpha$ -channeling can be implemented by launching waves which damp upon reaching an ion-cyclotron resonance layer. If, in turn,  $\xi \ll 1$ , then excitation of a weakly damped mode trapped in the device core is necessary. It is the latter case that is considered in this work.

- 
- [1] T. Intrator, S. Meassick, J. Browning, R. Majeski, J. R. Ferron, and N. Hershkowitz, *Nucl. Fusion* **29**, 377 (1989).
- [2] Y. Amagishi, A. Tsushima, and M. Inutake, *Phys. Rev. Lett.* **48**, 1183 (1982).
- [3] Y. Yamaguchi, M. Ichimura, H. Higaki, S. Kakimoto, K. Nakagome, K. Nemoto, M. Katano, H. Nakajima, A. Fukuyama, and T. Cho, *Plasma Phys. Control. Fusion* **48**, 1155 (2006).
- [4] Y. Yasaka, H. Takeno, A. Fukuyama, T. Toyoda, M. Miyakita, and R. Itatani, *Phys. Fluids B* **4**, 1486 (1992).
- [5] Y. Yamaguchi, M. Ichimura, H. Higaki, S. Kakimoto, K. Horinouchi, K. Ide, D. Inoue, K. Nakagome, and A. Fukuyama, *J. Plasma Fusion Res. Ser.* **6**, 665 (2004).
- [6] K. Yatsu, T. D. Akhmetov, T. Cho, M. Hirata, H. Hojo, M. Ichimura, K. Ishii, A. Itakura, Y. Ishimoto, I. Katanuma, J. Kohagura, Y. Nakashima, T. Saito, Y. Tatematsu, and M. Yoshikawa, *the Proceedings of the 28th EPS Conference on Controlled Fusion and Plasma Physics*, Funchal, Portugal, 2001 (The European Physical Society, Geneva, 2001), Vol. 25A, p. 1549.
- [7] R. I. Pinsky, *Phys. Plasmas* **8**, 1219 (2001).
- [8] R. W. Clark, D. G. Swanson, P. Korn, F. Sandel, S. Robertson, and C. B. Wharton, *Phys. Fluids* **17**, 1322 (1974).
- [9] W. C. Turner, *J. Phys. Colloques* **38**, C6-121 (1977).
- [10] R. Majeski, J. J. Browning, S. Meassick, N. Hershkowitz, T. Intrator, and J. R. Ferron, *Phys. Rev. Lett.* **59**, 206 (1987).
- [11] Hogun Jhang, S. G. Lee, S. S. Kim, B. H. Park, and J. G. Bak, *Phys. Rev. Lett.* **95**, 035005 (2005).
- [12] J. Kesner, *Nucl. Fusion* **19**, 108 (1979).
- [13] R. Breun et al., *Phys. Rev. Lett.* **47**, 1833 (1981).
- [14] C. Riccardi, M. Fontanesi, A. Galassi, and E. Sindoni, *Il Nuovo Cimento D* **16**, 505 (1994).
- [15] H. Sugai, H. Kojima, and T. Okuda, *Phys. Lett. A* **92**, 392 (1982).
- [16] G. A. Wurden, M. Ono, K. L. Wong, *Phys. Rev. A* **26**, 2297 (1982).
- [17] C. Riccardi, P. Cantu, and M. Fontanesi, *Plasma Phys. Control Fusion* **37**, 885 (1995).
- [18] N. J. Fisch and J. M. Rax, *Phys. Rev. Lett.* **69**, 612 (1992).

- [19] N. J. Fisch, *Rev. Mod. Phys.* **59**, 175 (1987).
- [20] N. J. Fisch and M. C. Herrmann, *Nucl. Fusion* **34**, 1541 (1994).
- [21] N. J. Fisch, *Phys. Plasmas* **2**, 2375 (1995).
- [22] N. J. Fisch and M. C. Herrmann, *Nucl. Fusion* **35**, 1753 (1995).
- [23] M. C. Herrmann and N. J. Fisch, *Phys. Rev. Lett.* **79**, 1495 (1997).
- [24] N. J. Fisch, *Phys. Rev. Lett.* **97**, 225001 (2006).
- [25] N. J. Fisch, *Fusion Sci. Technol.* **51**, 1 (2007).
- [26] A. J. Fetterman, N. J. Fisch, *Phys. Rev. Lett.* **101**, 205003 (2008).
- [27] T. K. Fowler and M. Rankin, *J. Nucl. Energy, Part C* **8**, 121 (1966).
- [28] D. A. Gates, N. N. Gorelenkov, and R. B. White, *Phys. Rev. Lett.* **87**, 205003 (2001).
- [29] R. G. L. Vann, H. L. Berk, and A. R. Soto-Chavez, *Phys. Rev. Lett.* **99**, 025003 (2007).
- [30] H. L. Berk, *Transp. Theory Stat. Phys.* **34**, 205 (2005).
- [31] H. L. Berk, C. J. Boswell, D. Borba, A. C. A. Figueiredo, T. Johnson, M. F. F. Nave, S. D. Pinches, and S. E. Sharapov, *Nucl. Fusion* **46**, S888 (2006).
- [32] S. D. Pinches, H. L. Berk, D. N. Borba, B. N. Breizman, S. Briguglio, A. Fasoli, G. Fogaccia, M. P. Gryaznevich, V. Kiptily, M. J. Mantsinen, S. E. Sharapov, D. Testa, R. G. L. Vann, G. Vlad, F. Zonca and JET-EFDA Contributors, *Plasma Phys. Contr. Fusion* **46**, B187 (2004).
- [33] A. I. Zhmoginov and N. J. Fisch, *Phys. Plasmas* **15**, 042506 (2008).
- [34] E. J. Valeo and N. J. Fisch, *Phys. Rev. Lett.* **73**, 3536 (1994).
- [35] T. H. Stix, *Waves in Plasmas* (Springer-Verlag, New York, 1992).
- [36] J. Pratt and W. Horton, *Phys. Plasmas* **13**, 042513 (2006).
- [37] J. Pratt, W. Horton, and H. L. Berk, *Journal of Fusion Energy* **27**, 91 (2008).
- [38] A. J. Lichtenberg and M. A. Lieberman, *Regular and Chaotic Dynamics* (Springer-Verlag, New York, 1992).
- [39] G. R. Smith and B. I. Cohen, *Phys. Fluids* **26**, 238 (1983).
- [40] G. R. Smith and A. N. Kaufman, *Phys. Fluids* **21**, 2230 (1978).
- [41] Y. Kiwamoto et al., *Plasma Phys. Control. Fusion* **39**, A381 (1997).

The Princeton Plasma Physics Laboratory is operated  
by Princeton University under contract  
with the U.S. Department of Energy.

Information Services  
Princeton Plasma Physics Laboratory  
P.O. Box 451  
Princeton, NJ 08543

Phone: 609-243-2750  
Fax: 609-243-2751  
e-mail: [pppl\\_info@pppl.gov](mailto:pppl_info@pppl.gov)  
Internet Address: <http://www.pppl.gov>